Precipitation Characteristics and Changes

2

Hengchun Ye, Daqing Yang, Ali Behrangi, Svetlana L. Stuefer, Xicai Pan, Eva Mekis, Yonas Dibike, and John E. Walsh

Abstract

Precipitation over the Arctic region plays a significant role in the water and energy cycle that sustains the Arctic's unique ecosystem. Although a cold climate with strong seasonality in temperature and moisture predominates, there is large spatial variation due to the heterogeneity of the landscape and atmospheric processes that control local weather and climate. Long-term historical synoptic records exist for some regions providing very valuable information on how precipitation has been changing, yet there are many challenges to overcome. Inconsistency in instrumentation and measurement techniques, undercatch due to weather conditions and precipitation types,

H. Ye (✉)
College of Natural and Social Sciences, California State University, 5151 State University Drive, Los Angeles, CA 90032, USA
e-mail: hye2@calstatela.edu

D. Yang · Y. Dibike
Environment and Climate Change Canada, Watershed Hydrology and Ecology Division, Victoria, BC, Canada
e-mail: daqing.yang@canada.ca

Y. Dibike
e-mail: yonas.dibike@canada.ca

A. Behrangi
Department of Hydrology and Atmospheric Sciences and Department of Geosciences, University of Arizona, Tucson, AZ, USA
e-mail: behrangi@email.arizona.edu

S. L. Stuefer
Water and Environment Research Center, University of Alaska Fairbanks, Fairbanks, AK, USA
e-mail: sveta.sturfer@alaska.edu

D. Yang and D. L. Kane (eds.), *Arctic Hydrology, Permafrost and Ecosystems*,
https://doi.org/10.1007/978-3-030-50930-9_2

uneven spatial and temporal distribution of station locations, and the reliability of remote sensing products all have to be considered. Research on Arctic precipitation is mostly focused on a specific continent or geographical or political region using very diverse perspectives and approaches. Here we draw from many of these and remote sensing to piece together studies that illustrate a broader picture of Arctic precipitation conditions and reveal emerging and/or diverging patterns of change. This chapter will (1) introduce existing and forthcoming sources of data and their corresponding challenges across the Arctic; (2) describe the distribution of precipitation characteristics including total amount, intensity, and frequency over major land areas and the oceans; and (3) demonstrate past changes and future predictions in these precipitation characteristics and their extremes. This will provide a fairly comprehensive knowledge repository and a strong foundation to promote and inspire future research development on precipitation over the Arctic region.

2.1 Introduction

Arctic precipitation is one of the main drivers of terrestrial Arctic hydrologic processes. With rapid warming in high latitudes, major changes in water and energy cycles and ecosystem of the region are expected, sometimes with greater amplitude due to the unique feedbacks in the cryosphere environment (e.g., Lau et al. 2013; Smith et al. 2005; Solomon 2007; Stuefer et al. 2017; Ye et al. 2016a). Arctic precipitation is also a principal source of feedback within the climate system as the albedo contrast between snow-covered and snow-free surfaces affects the surface energy balance and resulting hydrologic processes. Snow can also be an efficient thermal isolator separating the underlying surface from the atmosphere above, and thus, for example, determining the conditions for persistence or decay of permafrost. In addition, other cryospheric components, such as sea ice, can also play a role in precipitation feedback. For example, a decrease in sea ice would cause an

X. Pan
Institute of Soil Science, Chinese Academy of Sciences, Nanjing, China
e-mail: xicai.pan@issas.ac.cn

E. Mekis
Environment and Climate Change Canada, Meteorological Research Division, Toronto, ON, Canada
e-mail: eva.mekis@canada.ca

J. E. Walsh
International Arctic Research Center, University of Alaska, Fairbanks, AK, USA
e-mail: jewalsh@alaska.edu

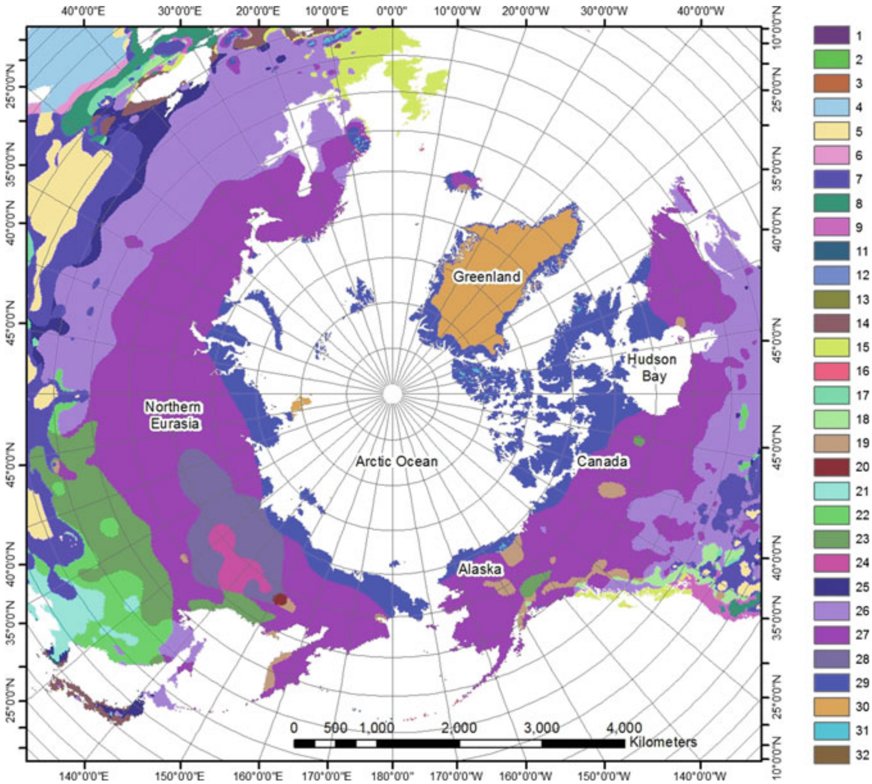

Fig. 2.1 Köppen's climate regimes north of 45° N based on Peel et al. (2007) updated dataset. Color codes used in this chapter are BWk (5), Cfb (15), Dsc (19), Dwc (23), Dwd (24), Dfa (25), Dfb (26), Dfc (27), Dfd (28), ET (29), and EF (30)

increase in Arctic precipitation because of the potential for increased local evaporation (Kopeca et al. 2015).

The largest continuous land surface over the Arctic north of 45° N is northern Eurasia, followed by Canadian territories and Alaska. The climate regimes are dominantly cold climate (D) with strong seasonality in moisture and temperature. Based on Koppen's classification updated by Peel et al. (2007) the climate includes cold-without dry season-cold summer (Dfc) over northern areas, cold-without dry season-warm summer over southern areas (Dfb), and Tundra (ET) along the arctic coast and high elevations (Fig. 2.1). Polar Frost (ET) climate prevails over Greenland. Along the west coast of Eurasia, it has temperate-without dry season-warm summer (Cfb) and other seasonal variations of cold climate along the west coast. Cold-winter dry-cold summer (Dwc), cold-winter dry-warm summer (Dwb), and cold-winter dry-hot summer (Dwa) are found over the east coast of northern Eurasia (Fig. 2.1). Cold dry-summer cold-winter (Dsc) climate class occurs in northern Canada and Alaska. There are also some patches of cold desert (BWk) over the southern edges of northern Eurasia and western Canada.

Historical precipitation records are available mostly from the former Soviet Union, Canada, Alaska, and northern European countries with varying data record lengths and distribution densities, thus most research has focused on these three large land areas. However, accurate measurements of precipitation are challenging due to the multiphases and wide range of intensity in this extreme environment (Rawlins et al. 2007). Researchers, engineers, stakeholders, and the general public need to be aware of the precipitation data biases and limitations.

2.2 Precipitation Data and Quality

Precipitation records over the Arctic region include historical synoptic weather stations or research stations operated by various governments and local agencies' monitoring sites, snow measurement stations using rulers or snow telemetry, drifting stations over the Arctic Ocean ice surface, and (in recent decades) remote sensing products. Each country has its own history and unique ways of collecting data, especially in earlier years. While surface station data have been available for more than a century, they can contain large errors in high latitudes for two main reasons: (1) the precipitation gauge network is often sparse and discontinuous in most regions (a substantial decrease in the number of high-latitude precipitation stations since 1990 has exacerbated this limitation) and (2) precipitation measurement must be bias-corrected to account for wetting loss and gauge undercatch due to strong wind and/or blowing snow (Goodison et al. 1998; Yang et al. 2001; Sturm and Stuefer 2013). The bias correction factors, which are largest for solid precipitation, can be as high as 300% (Fuchs et al. 2001) depending on the choice of correction method. Walsh et al. (2008) and others have found that estimates of Arctic regional mean precipitation from several observational sources show considerable scatter, and the observational estimates based on gauge-adjusted station data are considerably larger than other observational estimates. Thus different methods of bias correction have been developed for specific types of instrumentation and for different regions (Goodison et al. 1992). Moreover, for many stations, it may be necessary to join observations to produce longer time series of rainfall and snowfall for trend analysis due to stations' relocation. In order to avoid artificial discontinuity affecting the trend, adjustment using overlapping periods and/or homogeneity testing can be applied. The annual and seasonal trends before and after adjustments show that the trends computed from the adjusted data present a more consistent regional pattern than do trends computed from unadjusted observations (Vincent and Mekis 2009).

2.2.1 Historical Data of Surface Observations

Arctic Ocean

Drifting ice stations over the Arctic Ocean and adjacent Siberian seas was set up by the Russian Arctic and Antarctic Research Institute during 1950–1991. These operated ice camps reported position, surface weather, atmospheric soundings, solar radiation, and snow conditions. Observations were made throughout the Arctic basin with a spatial resolution dependent on the movement of the drifting ice floes on which the stations were located. At all the drifting stations, precipitation was measured using a shielded Tretyakov precipitation gauge mounted on a geodesic frame, with the orifice at 2 m high. Measurements were made at 0600 and 1800 h (local time) using the volumetric method (Colony et al. 1998).

The Tretyakov gauges were tested against the WMO reference at 11 stations in 7 countries. The intercomparison data collected at these sites for more than 3 winter seasons represent a great variety of climate, terrain, and exposure. The relationship of Tretyakov gauge catch efficiency to wind speed and air temperature was developed by Yang et al. (1995) and Goodison et al. (1998) and has been used to improve data accuracy. The majority of the drifting station data were collected in climatologically uniform regions (Colony et al. 1998), since the ice stations tended to be clustered in the central part of the Arctic Ocean (Fig. 2.2) (Yang 1999). Figure 2.3 presents the overall mean monthly gauge-measured precipitation and bias corrections for the drifting stations operated from 1957 to 1990 (Yang 1999). It shows that monthly gauge-measured precipitation ranged from 5 to 20 mm, with the minimum in April and the maximum in July. Monthly correction for wind-induced undercatch varied from 3 to 11 mm, or about a 20–100% increase in the gauge-measured amounts. The relative increase of monthly precipitation (ratio of monthly correction to monthly measured value) is much higher in the cold season (September to May) than in the warm season (June to August), mainly due to the higher wind-induced gauge undercatch for snow and also the smaller amount of absolute precipitation in the cold season. Overall, monthly precipitation was increased by 50–90%, i.e., from 5–20 mm to 10–30 mm, due to the bias correction; it was even doubled for winter months of low precipitation.

The seasonal cycle of the bias-corrected precipitation is different from the gauge-measured data. The monthly maximum shifted from July to September; this seasonal pattern was reported by Legates and Willmott (1990) and is also in general agreement with most GCM simulations (Walsh et al. 1998). Quantitatively, the amount of the bias-corrected monthly precipitation is lower than Legates and Willmott (1990) for most of the months; this discrepancy may have been caused by using different datasets and by the different bias correction methods applied in the studies.

Annual corrections for wind-induced biases ranged from 50 mm to 170 mm and the annual correction for trace precipitation events varied from 10 mm to 30 mm. The bias correction raised the annual precipitation to 200–500 mm (from 100 mm–300 mm based on gauge records) for the drifting stations, an increase of 40–90%;

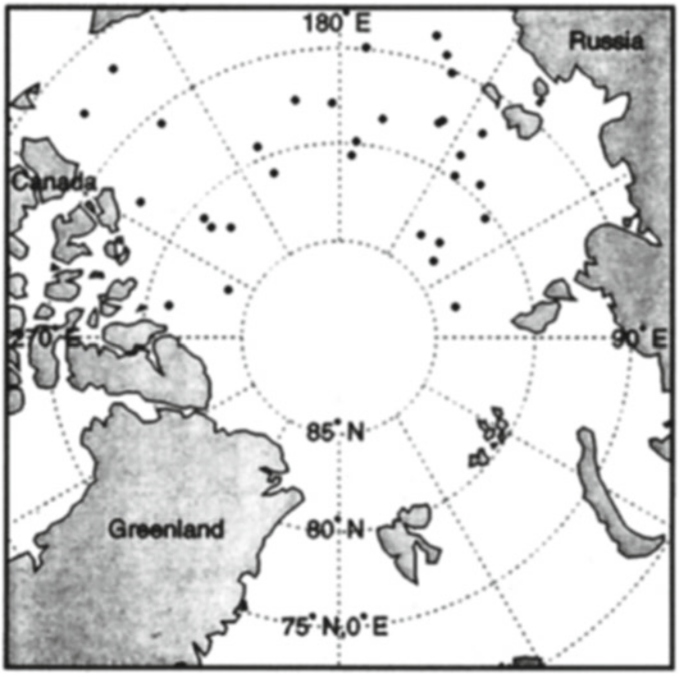

Fig. 2.2 Annual mean position of the Arctic Ocean drifting stations during 1957–1990 (Yang 1999)

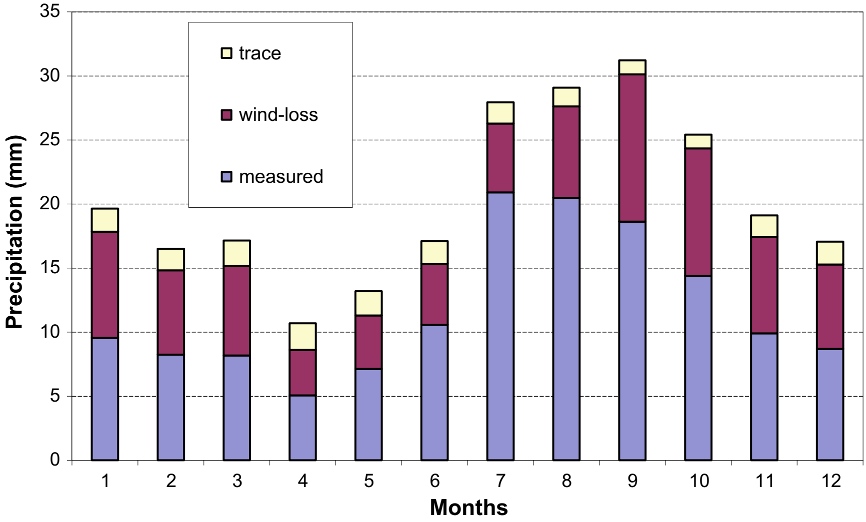

Fig. 2.3 The overall mean monthly gauge-measured precipitation and bias corrections for all drifting stations during 1957–1990 (Yang 1999)

consequently, the long-term mean annual precipitation is estimated to be 260 mm (from 150 mm) for the Arctic Ocean.

Alaska

Unlike other regions, precipitation data collection networks in Alaska were concurrently developed by different agencies to address each agency's specific needs and projects (Kane and Stuefer 2015). The precipitation data in Alaska were primarily collected by (1) the National Oceanic and Atmospheric Administration (NOAA) National Weather Service (NWS), (2) the NRCS Snow Telemetry (SNOTEL), (3) the United States Geological Survey (USGS), and (4) the Alaska Department of Transportation and Public Facilities (ADOT&PF). In addition to federal and state agencies, private industry and academia collect precipitation data in remote regions for environmental research projects. Each agency has its own protocol and site configurations for precipitation data collection. The use of collected precipitation data for climate change research was not a priority (or consideration) at the time when these networks were established. More recent initiatives, such as NOAA's U.S. Climate Reference Network (USCRN), were designed to fill the gap and support climate change research. The current USCRN network includes 21 first-order NWS stations in Alaska, which are commonly used for climate research.

Canada

The National Climate Data Archive of Environment Canada has daily rainfall gauge and snowfall ruler data. The Meteorological Service of Canada (MSC) has used a number of different gauges for measuring rainfall over the past 150 years (Metcalfe et al 1997). There are two Adjusted Precipitation for Canada-Daily datasets, the APC1-Daily, introduced in mid-1990 and the APC2-Daily, the second generation that extended the datasets to 2007 in order to provide more accurate precipitation amounts for trend analyses (Mekis and Vincent 2011a, b).

Precipitation accumulation with less than 1 mm has issues with quality due to a significant amount of trace precipitation which was not consistently defined, for example, difficulty in observation, conversion on metric system around 1977–78, etc. (Mekis 2005; Mekis and Vincent 2011a, b). Fresh snowfall measured with snow ruler in Canada adds another layer of complexity to the observations due to the spatial and temporal variation of snow water equivalent. Adjustment factors for snow density variation ranging from more than 1.5 over the Maritimes to less than 0.8 over southern-central British Columbia (Mekis and Brown (2010), allow estimates of SWE for all long-term climate stations in Canada.

Northern Eurasia

The network of stations in Russia began with 23 sites in 1850 and grew to 552 primary and secondary observing stations (including Finland and Poland) in 1890 (Groisman et al. 1991). There were 11,000 stations measuring precipitation during the 1980s over the USSR but these decreased drastically in the following decades. There were changes in gauges, installation standards, measurement practices, and relocation of stations that occurred at different times. Bias correction methods were developed to minimize the impact of these changes (Groisman et al. 1991; Groisman and Rankova 2001). The monthly precipitation records of 622 stations are available for international users from the National Snow and Ice Data Center, Boulder, Colorado (Ye 2001; Serreze and Etringer 2003).

Precipitation daily record data over Russia were collected by the Russian Federal Service for Hydrometeorology and Environmental Monitoring (Roshydromet). Post-processing was done by the All-Russian Institute for Hydrometeorological Information and is also available from the NOAA data archive. An earlier version is available from the Carbon Dioxide Center (Bulygina and Razuvaev 2012). Again, the changes in precipitation gauge types and observation practices may have impacted the quality of the data. Various quality control methods were used depending on their instruments and observation practices to adjust for undercatch in solid and liquid precipitation measurements. Overall, the quality of data for climate change study is better starting in 1966 due to the consistency of instrumentation and quality control methods (Groisman et al. 1991). The most commonly used dataset available is the daily precipitation data from Daily Temperature and Precipitation Data for 518 Russian Meteorological Stations archived at the Carbon Dioxide Information Analysis Center (Bulygina and Razuvaev 2012).

Pan-Arctic

Uncertainties exist in the estimation of precipitation climatology over the high-latitude regions mainly due to sparse observation networks, space-time discontinuities of precipitation data, and biases of gauge observations. Of these factors, biases in gauge measurements, such as wind-induced undercatch, wetting loss (water adhesive to the surface of the inner walls of the gauge that cannot be measured by the volumetric method), evaporation loss (water lost by evaporation before the observation is made), and underestimation of trace precipitation amounts (Goodison et al. 1998), are particularly important, because they affect all types of precipitation gauges, especially those used in the cold regions. The WMO experiment has developed bias correction procedures for many precipitation gauges commonly used around the world, including those used in the high-latitude countries (Goodison et al. 1998). These bias correction methods have been applied in the high-latitude regions (including the Arctic Ocean drifting station records) and resulted in significantly higher estimates of precipitation (Yang et al. 1998; Yang 1999). Based on the regional applications of the WMO bias correction methods, Yang et al. (2005) expanded the analyses to the pan-Arctic scale, using available long-term daily data collected at locations above 45° N across national boundaries. The major advantage of this approach is the capability of examining the discontinuity of precipitation records across national borders.

Bias corrections for the observed daily precipitation over northern land have been conducted using daily meteorological data of precipitation, temperature, and wind speed. A consistent bias correction procedure was applied to quantify the biases of wind-induced undercatch, wetting losses, and trace precipitation amount on a daily basis. Its impacts on the precipitation climatologies were investigated by using a subset of the global daily data, 4802 stations located north of 45° N with data records longer than 15 years during 1973–2004.

The corrections have increased the gauge-measured monthly precipitation significantly by up to 22 mm for winter months and by about 10 mm during the summer season. Wind-induced gauge undercatch is the largest error, but wetting loss and trace precipitation are also important particularly in the low precipitation regions. Relatively, the correction factors (CF = corrected/measured precipitation) are small in summer (less than 10%) and very large in winter (up to 80–120%) because of the increased effect of wind on gauge undercatch of snowfall. The CFs also vary over space, particularly in the snowfall season. The spatial patterns of CF are different from the measured and corrected precipitation especially in winter, with low CFs (20–40%) over the higher mid-latitudes and very high values (over 100%) along the windy Arctic coasts of low precipitation. Significant CF differences were also found across the USA/Canada borders mainly due to difference in catch efficiency between the national standard gauges. This inconsistency affects climate analyses over large regions, such as the Arctic as a whole (Fig. 2.4).

The impact of bias corrections on long-term precipitation changes over the northern regions was examined by calculating monthly trends for measured and corrected precipitation for the selected stations with records longer than 25 years during 1973–2004. Bias corrections generally enhance the long-term trends of monthly precipitation—indicating underestimation of precipitation changes,

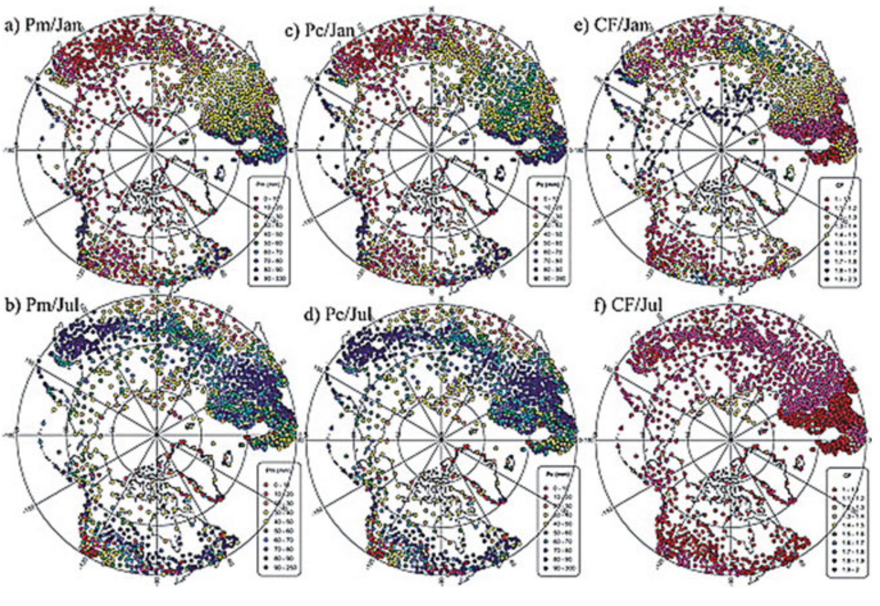

Fig. 2.4 Monthly mean gauge-measured (Pm) and bias-corrected (Pc) precipitation, and correction factor (CF) for January and July (Yang et al. 2005)

particularly for the regions with large changes, over the northern regions. These results clearly point to a need to utilize bias-corrected precipitation estimates to provide a better understanding of the Arctic freshwater budget and its change.

2.2.2 Remote Sensing Precipitation Products

During the last four decades space-borne sensors have enabled precipitation estimation with full areal coverage that can complement point measurements by gauge stations. Furthermore, they can provide complete coverage over both land and ocean, the latter of which is impossible through in situ network. However, remote sensing estimates also contain large uncertainties, especially in high latitudes where they still do not cover the entire high latitudes (e.g., Behrangi et al. 2012). Nevertheless, remote sensing of precipitation is an active area of research and development and significant progress has been made by improving both sensors and retrieval methods (e.g., Skofronick-Jackson et al. 2017).

Overall, four major types of sensors for precipitation estimation are infrared (IR) and microwave (MW) imagers and sounders, and more recently radars. IR data often lack a strong correlation with precipitation at fine spatiotemporal scales and show major limitations, especially for warm rain events (Behrangi et al. 2009). MW-based precipitation retrieval is more physical than IR-based as MW sensors sense hydrometeors in the entire atmosphere and capture bulk emission from liquid water at low frequencies and scattering by ice particles at high frequencies (Wilheit 1986). However, challenges such as insufficient sensitivity of sensors to light rain and snowfall, poor understanding of precipitation microphysics, unknown surface emissivity over snow and frozen land (Ferraro et al. 2013), problems in distinguishing light rain from clouds (Berg et al. 2006; Lebsock and L'Ecuyer 2011), and dependence of retrievals on prior knowledge of precipitation phase (Liu 2008) pose difficulties in MW-based retrieval of precipitation in high latitudes (Petty 1997). Radars typically provide the most direct and fine-scale observation of precipitation intensity. The 13.8 GHz Precipitation Radar (PR) aboard the Tropical Rainfall Measuring Mission (TRMM; Kummerow et al. 1998) has allowed advanced retrievals of moderate to intense rainfall over tropics (37° S–37° N) since 1997. However, it has no coverage in high latitudes and its sensitivity ($\sim$17 Dbz) makes it poorly suited to retrieve light rain and snowfall (Short and Nakamura 2000; Behrangi et al. 2012).

Combining multiple sensors (e.g., IR, MW) aboard multiple platforms is a popular means to enhance accuracy or spatiotemporal resolution of precipitation estimates (e.g., Hsu et al. 1997; Sorooshian et al. 2000; Kuligowski 2002; Huffman et al. 2007; Behrangi et al. 2010). Due to lack of quality precipitation products and geographical coverage of geostationary IR, several of the current combined products do not cover regions poleward of latitude 60 or 65 degrees in both hemispheres. The most popular combined products with global (90° S–90° N) coverage are (1) the Global Precipitation Climatology Project (GPCP; Huffman et al. 1997; Adler et al. 2003, 2016) which uses a combination of space-borne sensors over land

and ocean and gridded in situ observations from the Global Precipitation Climatology Centre (GPCC; Schneider et al. 2017) for monthly bias adjustment over land, and (2) the Climate Prediction Center (CPC) Merged Analysis of Precipitation (CMAP) product (Xie and Arkin 1997) which provides gridded global monthly estimates of precipitation using many of the same datasets as GPCP, plus Microwave Sounding Unit data. Furthermore, the method of merging the individual data sources in CMAP is different from GPCP.

During the last 15 years several new capabilities have emerged that can help improve retrieval of precipitation in high latitudes. These are mainly the launch and operation of CloudSat (Stephens 2008), the Global Precipitation Measurement (GPM) mission (Skofronick-Jackson et al. 2017), and the Gravity Recovery and Climate Experiment (GRACE) (Tapley et al. 2004).

CloudSat

The 94 GHz (W band) Cloud Profiling Radar (CPR) aboard CloudSat with a minimum detectable signal of ~−28 dBZ was launched in 2006. The high sensitivity of CloudSat allows for detection and estimation of light rainfall, drizzle, and snowfall that is often missed by other sensors (Behrangi et al. 2012, 2014a) thus CloudSat has enabled assessing the performance of several existing products in high latitudes. Figure 2.5 shows the contribution of light precipitation to total precipitation occurrence and amount over high-latitude ocean in the Northern Hemisphere. For example, it shows that at 65° N and higher latitudes, more than 70% of total precipitation occurs at intensities less than 0.5 mm/hr which sum up to about 15% and 40% of total precipitation amount at ~65° N and 80° N,

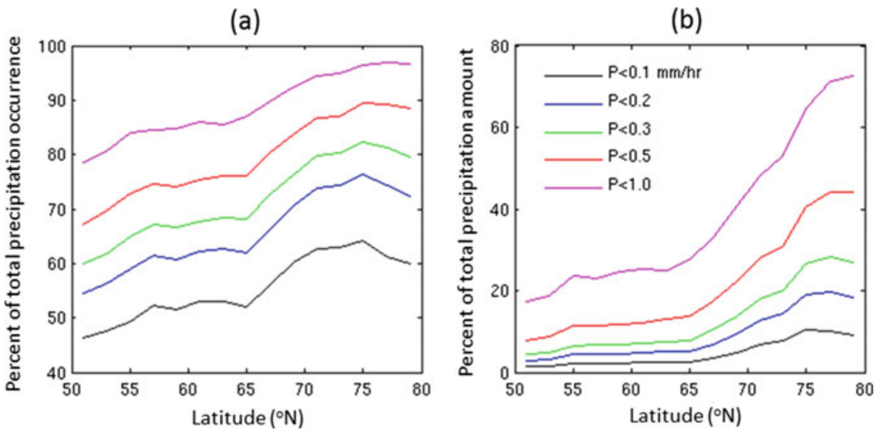

Fig. 2.5 Contribution of light precipitation to **a** total precipitation occurrence and **b** total precipitation amount over high-latitude ocean. Light precipitation is defined as precipitation rate below threshold P shown in legend of panel (**b**). Precipitation rates are obtained by accumulating rain, mixed phase, and snow intensities from four years (2007–2010) of CloudSat rain and snow products

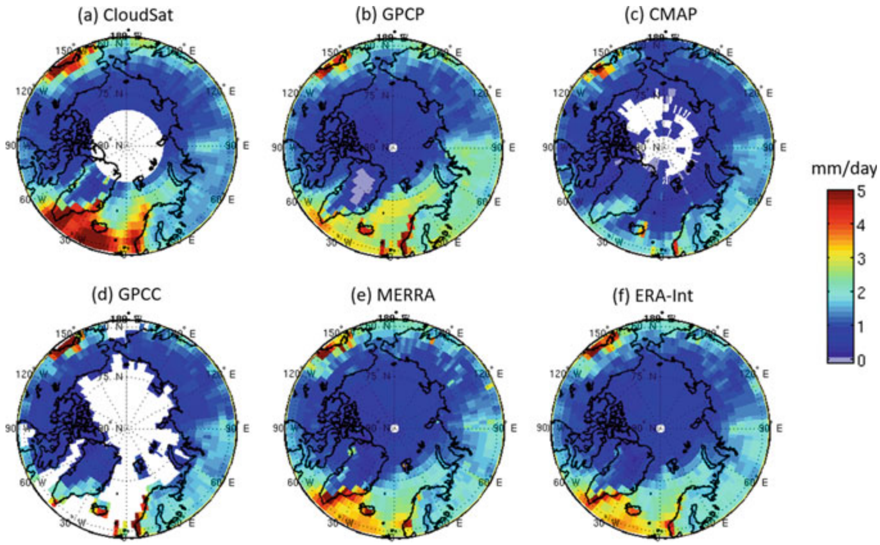

Fig. 2.6 Maps of four-year (2007–2010) averaged precipitation rates (mm/day) constructed from CloudSat, GPCP, CMAP, GPCC, MERRA, and ERA-Interim over land and ocean north of latitude 57°. Missing or non-reported data are shown in white. The figure is from Behrangi et al. (2016) with modifications

respectively. Note that 0.5 mm/hr typically exceeds the sensitivity of most of the precipitation sensors prior to CloudSat.

Figure 2.6 shows maps of four-year (2007–2010) averaged precipitation rates (mm/day) north of latitude 57° N constructed from CloudSat, GPCP, CMAP, GPCC, and two popular reanalysis products: the Modern-Era Retrospective Analysis (MERRA; Bosilovich et al. 2011) and European Center for Medium-Range Weather Forecasting (ECMWF) global atmospheric reanalysis (ERA-Interim; Dee et al. 2011). GPCC is based on gauge observations so reports no ocean data, suggesting that satellite data is critical to fill the observational gaps. Despite the general agreement in their seasonal patterns, several interesting features can be observed from Fig. 2.6. For example, based on CloudSat estimates, the highest precipitation rates are in the North Atlantic up to the coast of Greenland and along the southern coast of Alaska. This is not clearly seen in GPCP and CMAP. Furthermore, over the Atlantic south of 70° N, CloudSat reports average precipitation about or greater than 5 mm/day and shows a noticeable precipitation gradient around 70° N over the Atlantic Ocean. These features are not well produced in GPCP and reanalysis show less precipitation intensity than CloudSat.

Table 2.1 shows the annual (2007–2010) precipitation rates from the products shown in Fig. 2.6, separately over land and ocean. As can be seen GPCC has the lowest and GPCP has the highest annual rates. GPCC full product used here does not include gauge corrections, while GPCP uses a gauge correction based on the

Table 2.1 Summary of annual (2007–2010) precipitation rate of products over land and ocean north of latitude 57° (shown in Fig. 2.6)

Products	Annual precipitation rate (mm/year)	
	NH land	NH ocean
CloudSat	478	684
GPCP	557	692
CMAP	433	330
GPCC	447	_
MERRA	553	653
ERA-Interim	528	641

Legates climatology (Legates and Willmott 1990) that may result in overestimation of precipitation, especially over Eurasia and western Siberia, based on previous studies (Behrangi et al. 2014b, 2016). Furthermore, in estimating precipitation from CloudSat, an experimental product is used for rainfall over land.

GPM

The GPM core observatory satellite was launched in February 2014 and carries two important instruments for precipitation estimation: (1) the Dual-frequency Precipitation Radar (DPR) with Ku/Ka (13.6/35.5 GHz) bands and (2) the GPM Microwave Imager (GMI) which has 13 channels with frequencies ranging from 10 to 183 GHz (Draper et al. 2015). These instruments cover ~60° S-N, extending TRMM's coverage (~37° S-N) to higher latitudes. The better sensitivity of the GPM DPR (~0.2 mm/hr) relative to the single Ku frequency TRMM PR (~0.5 mm/hr), four additional high-frequency channels on the GMI, and advanced retrieval techniques (Kummerow et al. 2015, 2016) have added new capabilities to detect and quantify snowfall and rainfall everywhere, including polar regions. This is an important advancement, as the Passive Microwave precipitation retrievals used to be significantly low or missing over frozen surfaces in the pre-GPM era (Behrangi et al. 2014a). Initial analysis of the latest GPM products have shown that the accuracy of GPM PMW products has improved in high latitudes (Kummerow et al. 2016). It should be noted that the products are currently under development and evaluation. In the near future the products will not only include the GPM post-launch era, but will also be available for earlier periods by applying the latest retrieval methods to the constellation of low Earth-orbiting sensors.

GRACE

The GRACE mission (Tapley et al. 2004) has retrieved mass variations within the Earth with high accuracy since 2002. Recent studies have shown that GRACE observations are valuable for precipitation estimation in cold regions (Swenson 2010; Boening et al. 2012; Behrangi et al. 2017). Precipitation accumulation can be calculated using GRACE Terrestrial Water Storage Anomaly (TWSA) estimates based on the mass conservation principle, dictating that any change in one component of the water balance must be compensated for by the same amount collectively in the other components (e.g., Dingman 2008). The application of this concept over cold regions in high latitudes can leverage recent advances in estimating TWSA from GRACE (e.g., through mascons solution; Watkins et al. 2015), low uncertainties in remotely sensed ET in cold regions, and runoff observations to provide observational constraints on basin- and grid-level precipitation estimates. By applying this method over Eurasia, Behrangi et al. (2016) showed that GPCP precipitation rates over Eurasia are almost twice those estimated by CloudSat and GRACE. This is consistent with previous findings of Behrangi et al. (2014b; via water vapor convergence) and Swenson (2010), and is likely related to overcorrection for gauge undercatch in GPCP. This overestimation can also be seen in Fig. 2.6. Behrangi et al. (2017) also used a similar concept and compared GRACE-based precipitation accumulation with GPCP and a few other products over large endorheic basins in the Tibetan Plateau. While the results matched fairly well in summer, GPCP showed ~30% bias compared to GRACE estimates in winter, when accurate precipitation retrieval is more difficult. It was also shown that GRACE can provide valuable insights on gauge undercatch correction factors that otherwise are often difficult to assess (Behrangi et al. 2018).

2.3 Precipitation Characteristics Over the Arctic

Due to extremely low air temperatures, trace precipitation (less than the minimum measurable amount for a given gauge) is very common (Yang et al. 1988). Thus, accounting for trace precipitation is important over vast parts of the Arctic, where precipitation amounts are very low and the sum of all trace amounts becomes a significant portion of total precipitation. Including trace events may increase the amount of precipitation by up to an additional 20% (Mekis 2005). The number of days with precipitation below 1 mm is averaged at about 51 and 69% of total wet days in winter and summer respectively and contributes to about 13 and 5.2% of their corresponding seasonal precipitation total on average.

Precipitation estimates in terrestrial Arctic regions vary from over 1,000 mm at the southern coast of Greenland, western Scandinavia, and the northeastern Pacific with amounts decreasing to about 300 mm in Northern Siberia and Northern Canada to the lowest total precipitation of <150 mm over Northern Greenland and the northern Canadian Arctic archipelago (Serreze and Hurst 2000). Over the Arctic Ocean, annual precipitation is estimated to be 260 mm (about 60–100% in snow), based on records from drifting stations after bias corrections increases 40–90%; Yang et al.1995; Goodwin et al. 1988).

In addition, there is very strong seasonality in precipitation characteristics over the Arctic given the large land coverage that consists of diverse climate regimes. For example, over Northern Eurasia, precipitation is lowest in winter (about 84 mm), followed by spring (98 mm). The highest occurs in summer (205 mm), followed by fall (143 mm). In general, winter and spring precipitation shows a longitudinal pattern of wetter along both coasts and drier inland. Western European Russia receives about 150 mm and this decreases to about 100 mm in western

Siberia, 50 mm or lower over northeastern Siberia and then increases again along the coast of eastern Siberia (Fig. 2.7a, b). There is also a strong localized precipitation of up to 600 mm along the east shore of the Black Sea, possibly related to Lake Effect snow and orographic lifting (Korzun 1984; Lydolph 1977; Ye 2001, 2016a, b). Summer and fall precipitation have a latitudinal pattern of higher in the south and lower toward the north (Fig. 2.7c, d).

The number of wet days (including days with 0.1 mm or higher daily precipitation total) is highest in winter of up to 60 days or more over northern European Russia and northwestern Siberia. Fall has the second highest number of wet days and spatial patterns resembling that of the winter season (Fig. 2.7e, h). The area-averaged value is about 40 days in winter and fall. Spring and summer have

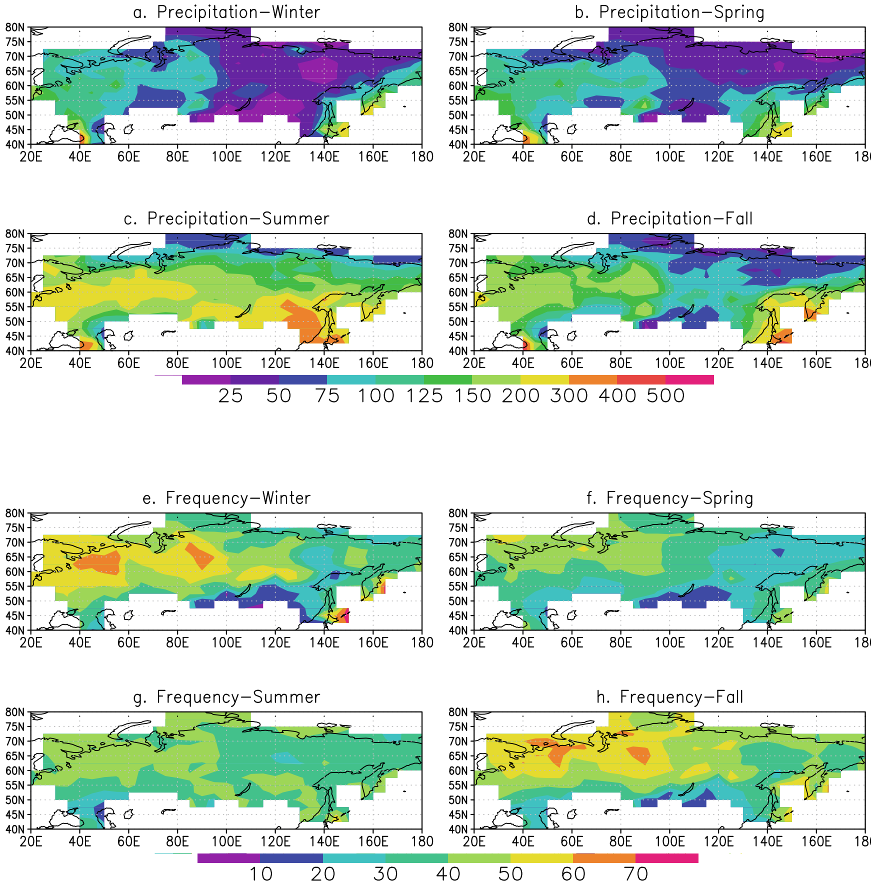

Fig. 2.7 Geographical distributions of seasonal precipitation total (mm) and frequency (wet days) based on 1966–2010 (Ye et al. 2016a)

similar distributions of low wet days of mean 32 days and 37 days respectively (Fig. 2.7f, g).

As a result, summer has the highest daily precipitation intensity of 5.4 mm/day with a well-defined zonal distribution decreasing toward the north, followed by the fall of 3.7 mm/day. Fall and spring have similar patterns of daily precipitation intensity distribution with spring having a slightly lower precipitation intensity of 3.0 mm/day. Winter has the lowest daily intensity of only 2 mm/day (Fig. 2.8). For all seasons, the highest intensities are found in the wet regions along the east shore of the Black Sea and along the southeastern coast near the Pacific Ocean. From Figs. 2.7 and 2.8, one can clearly see that there are very different precipitation characteristics between winter and summer. Winter precipitation is made up of very frequent low-intensity events while summer features more sporadic but intense precipitation. Spring and fall precipitation characteristics lie between those of winter and summer but with an evident zonal pattern more characteristic of summer precipitation intensity rather than the longitudinal pattern that characterizes winter precipitation intensity.

The entire state of Alaska is located north of 45° N, defined in this book as the southern boundary of the pan-Arctic hydrologic region. The climate within the state of Alaska ranges from maritime on Alaska's southeast coast to Arctic in the region north of the Brooks Range. Alaska is commonly separated into several climate zones that are useful in describing precipitation distribution across the state: Arctic, Interior, West Coast, Aleutians, Cook Inlet, and Alaska Southeast Coast (Shulski and Wendler 2007; Kane and Stuefer 2013).

Precipitation distribution in Alaska is controlled by the state's large geographic extent, proximity to the oceans, and extreme topographic gradients—from sea level to the highest peak of North America (Denali 6,190 m). Mean total precipitation

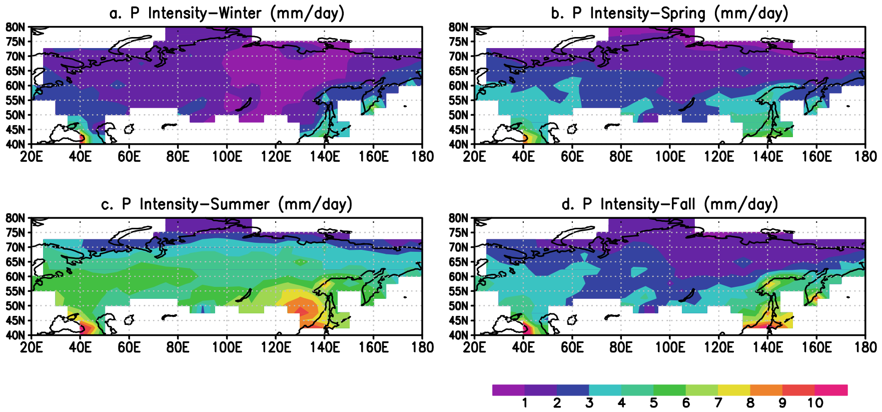

Fig. 2.8 Geographical distribution of mean seasonal precipitation intensity based on 1966–2010 (mm/day) (Ye et al. 2016a)

has large spatial variation from 3,000 mm in Alaska Southeast Coast to 250 mm in Arctic Coastal Plain (Kane and Stuefer 2013).

Precipitation frequency is much higher in the southern portions of the state in comparison to the Interior and Arctic regions. The mean annual statistics on the number of days with precipitation above 2.5 mm can serve as a metric that shows high variability in frequency across Alaska. For example, Barrow (Arctic) has 11 days a year with precipitation above 2.5 mm, 31 days for Fairbanks (Interior), and 143 days for Kodiak (Alaska Southeast Coast) (Shulski and Wendler 2007).

Seasonally, the frequency of precipitation (number of days with precipitation) in the Arctic and Interior Alaska regions is highest in July–August and lowest in April. The percentage of precipitation falling as solid on the Arctic Coastal Plain is on average about 60%, ranging from 40 to 88% (Stuefer and Kane 2016; Stuefer, Kane, and Liston 2013). The intensity of precipitation in Arctic Alaska is highest during summer months due to warmer air temperatures and ice-free coastal seas that allow air masses to hold more moisture (Shulski and Wendler 2007). Alaska Southeast Coast and Aleutians have extreme precipitation later in the year, during fall and winter. The largest 1-day precipitation event in Alaska—382 mm—was recorded on 10 October 1986 in Seward (Alaska Southeast Coast); this information supersedes the previous record for Angoon station (Brettschneider and Trypaluk 2014). For comparison, the largest 1-day precipitation event of 87 mm occurred in Fairbanks (Interior) on 12 August 1967 (Perica et al. 2012), resulting in historical flooding of Fairbanks and led to the construction of the flood control facilities around the city.

a. Changes in Precipitation Characteristics Based on Historical Records

Studies of observed precipitation trends in the terrestrial Arctic suggest that the magnitude and direction of trends very much depend on the specific region considered and the particular period of analysis. In general, warming over the Arctic region is associated with upward trends in total precipitation and extremes, however the magnitude and direction of trend may vary with the selected time period (e.g., Alexander et al. 2006; Bieniek et al. 2014; Tebaldi et al. 2006). It is estimated that total precipitation over the Arctic in the past century increased at a rate of about 1% per decade (ACIA 2005). The exception is for summer, when precipitation may have been decreasing in many regions (Dirmeyer et al. 2013; Ye et al. 2016a). The decrease is estimated at about 0.79 mm/year over the terrestrial pan-Arctic during 1989–2005 based on ERA-Interim data (Rawlins et al. 2010).

Canada has seen significant increases in precipitation, especially northern Canada including the Canadian Arctic Archipelago (Mekis and Vincent 2011a, b; Vincent et al. 2015; Rapaic et al. 2015). An increase in precipitation total in spring over British Columbia and the Canadian Prairies has been accompanied by increasing air temperature (Jarujareet 2016; Martin 2017). Although no significant changes in total wet days over British Columbia have been found, significant decreases in snowfall days and frozen rain days were found (Montenegro 2015). A study over Southeast Canada suggests that decreases in wet days during summer and fall occur as air temperature increases (Chamnansiri 2016).

Positive trend in total precipitation in Alaska Arctic Coastal stations was found during more recent decades 1981–2012 (Bieniek et al. 2014). During this period, an increase in October and November monthly precipitation was the most pronounced, i.e., November precipitation increase was 7.4 mm from 1981 to 2012.

Regional analysis of three gridded datasets (GPCC, CRU, and UDEL) in Alaska Arctic supports an increasing trend in total precipitation during 1980–2010 time period (McAfee et al. 2014). Total precipitation in Utqiaġvik (former Barrow, Arctic) shows no significant decrease during 1950–2010, (McAfee et al. 2013). Similarly, total change in mean accumulated precipitation in Utqiaġvik was reported as −1.7 mm from 1949 to 2012, with largest decrease of −2.3 mm observed in summer (Bieniek et al. 2014).

Precipitation total over Eurasia in general has been increasing in winter (Ye 2001) but not changing much in other seasons (Ye et al. 2016a). This is in general consistent with the observation that increasing atmospheric water vapor associated with higher air temperature is related to higher precipitation efficiency in winter and lower precipitation efficiency in summer (Ye et al. 2014).

Most evident is increasing precipitation extremes over Northern Eurasia (Groisman et al. 2005; Zolina et al. 2010). The daily intensity is about 1–3% per degree of air temperature increase in all seasons (Ye et al. 2015, 2016a) over northern Eurasia. Over Canada, 2/3 of regions have shown increases in extreme rainfall amount (Shephard et al. 2014). It appears that increasing higher intensity precipitation is accompanied by decreasing lower intensity precipitation (Ye et al. 2015).

Convective precipitation appears to be increasing at the expense of non-convective precipitation (Ye et al. 2016b, 2017). The transitional seasons of spring and fall have become summer-like by the late 1980s when occurrence of convective precipitation outnumbered non-convective precipitation (Ye et al. 2017). Increasing extremes and daily intensity are occurring in the convective precipitation events which are getting stronger and more frequent (Ye et al. 2017). Changes in atmospheric water vapor or specific humidity appear to be key to changes in precipitation characteristics (Ye and Fetzer 2009; Ye et al. 2014, 2017).

2.4 Extreme Precipitation: Case Studies

a. An Alaska Example in the twenty-first century

Extreme precipitation events can have major consequences for ecosystems, infrastructure, and humans. The frequency and intensity of extreme precipitation events have been increasing in much of the world, and the increase of the highest percentiles of daily precipitation amounts have exceeded the increases in the median amounts in many areas (IPCC 2013; USGCRP 2014). However, there have been few studies of extreme precipitation in the Arctic. A recent study (Lader et al. 2017) used regional dynamical downscaling with the Weather Research and Forecasting Model (WRF) to investigate projected twenty-first-century changes of extreme precipitation over Alaska. The forcing data used for the downscaling

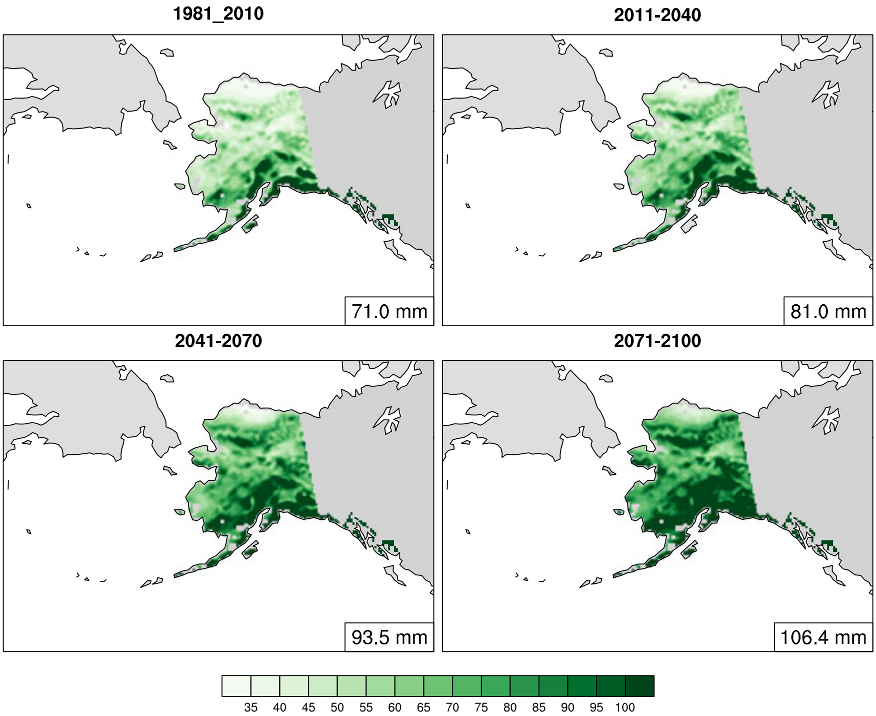

Fig. 2.9 30-year means of the annual maximum consecutive 5-day precipitation (mm). The statewide average is located at the bottom right

simulations included the ERA-Interim reanalysis and GFDL-CM3 climate model output for a historical period (1976–2005), and GFDL-CM3 RCP8.5 for the future (2006–2100). A quantile mapping procedure was used to bias-adjust the distributions of the daily precipitation simulated for a historical period.

In the model simulation, the statewide average of the annual mean accumulation increases from 79.3 cm yr^{-1} during the base period (1981–2010) to 121.2 cm yr^{-1} by 2071–2100 (Fig. 2.9), an increase of 53%. The changes to extreme precipitation are similarly dramatic. The average annual count of heavy precipitation days ($\geq$10 mm) and very heavy precipitation days ($\geq$20 mm) increases by 66% and 101%, respectively (Table 2.1). The average annual maximum 1-day (Table 2.1) and 5-day (Fig. 2.1) precipitation amounts are also projected to increase by more than 50% by the end of the century. The greatest relative change by percentage is expected for the Brooks Range and locations further north. The average annual maximum number of consecutive wet days ($\geq$1.0 mm) is projected to increase by 23%, whereas the number of consecutive dry days is projected to decrease by 21% (Table 2.1). This does not necessarily mean that the threat for severe drought would decrease, however, because higher temperatures would lead to greater daily evapotranspiration.

There is also an apparent connection between diminishing sea ice and extreme precipitation across western Alaska. The average daily sea ice extent during March, when the climatological maximum annual extent is reached, extends well south in the Bering Sea to between St. Paul Island and the Aleutians from 2011–2040, but this line recedes into the Chukchi Sea from 2071–2100. Coincident with these losses of sea ice is an increasing trend for greater extreme precipitation, first for the Aleutians and southwest Alaska from 2041–2070, and then for the Bering Strait and northwest Alaska from 2071–2100 (Table 2.2). Possible mechanisms for this relationship include shifting storm tracks and dynamics along the ice edge, and greater local evaporation in areas where sea ice has been replaced by open water (Kopec et al. 2015).

One of the few studies to examine corresponding trends in station data aggregated by climate divisions (Bieniek and Walsh 2017) did not find a significant increase in heavy precipitation events over Alaska during the 1920–2012 period. Similarly, Perica et al. 2012 reported lack of significant trends in annual precipitation maxima time series, used to update precipitation frequency estimates in the state of Alaska. This finding may well be a consequence of the precipitation measurement network, which is not only sparse over Alaska but is subject to the measurement errors and lack of bias-correction that limit the reliability of precipitation data for the Arctic (Yang et al. 2005).

b. Under Reporting of Daily $P_{\max}$

To investigate the impact of bias-correction on precipitation extremes, a subset of 1329 stations with over 15-year records within the period 1973–2004 were extracted from the bias-corrected daily precipitation dataset of Yang et al. (2005). A quality control was applied for extracting daily precipitation maximum in each year; a year was rejected if the fraction of missing data exceeded 5%.

The mean yearly gauge-measured daily maximum precipitation $Pm_{\max}$ at the sites ranges from 18 to 167 mm with a mean value of 53 mm over the northern regions. The spatial patterns of the mean values are characterized by low daily maximum precipitation in the near-polar region and west coast of Europe, moderate daily maximum precipitation along latitude 60ºN in Eurasia and along the lower latitude than 60° N in North America, and high daily maximum precipitation interspersing in the lower latitude than 60° N of Eurasia and the coasts of Pacific Ocean (Fig. 2.10a). Underestimation of the gauge-measured daily maximum precipitation over the northern regions is significant (Fig. 2.10b). The mean yearly corrected daily maximum precipitation $Pc_{\max}$ ranges from 20 to 185 mm with a mean value of 59 mm over the northern regions. Despite the general agreement in the spatial pattern of the gauge-measured daily maximum precipitation extremes, and the corrected precipitation extremes, several regional features can be identified in Fig. 2.10a, b. For example, the bias correction does not change the pattern of the precipitation extreme distribution, and the high precipitation maxima (>60 mm/d) are mainly concentrated in western northern Eurasia. The increased

Table 2.2 The median (Med), 90th percentile (90P), 99th percentile (99P), maximum (Max) and annual total of daily precipitation (mm) averaged over successive 30-year periods for the nearest downscaled grid cell to selected **cities** in Alaska. Values are for model grid cells containing stations

Station		Precipitation (mm)				
		Median	90th % ile	99th % ile	Max daily	Annual mean
Barrow	1981–2010	0.07	1.73	6.99	24.62	217.72
	2011–2040	0.10	2.06	8.04	30.67	263.93
	2041–2070	0.12	2.69	9.77	28.67	335.84
	2071–2100	0.19	3.58	12.28	34.68	439.88
Nome	1981–2010	0.06	4.66	17.47	43.43	541.55
	2011–2040	0.12	5.61	21.10	48.52	661.58
	2041–2070	0.15	7.02	25.23	62.91	825.44
	2071–2100	0.24	8.62	29.77	93.62	1022.17
McGrath	1981–2010	0.35	5.59	16.50	39.34	683.52
	2011–2040	0.50	6.36	18.72	50.56	794.53
	2041–2070	0.61	7.62	21.61	88.60	944.63
	2071–2100	0.65	7.82	25.02	90.53	1010.98
Fairbanks	1981–2010	0.18	4.02	13.62	45.37	495.86
	2011–2040	0.21	4.62	16.39	68.76	582.42
	2041–2070	0.26	5.48	18.80	97.92	696.25
	2071–2100	0.33	6.22	21.27	65.54	797.80
Anchorage	1981–2010	0.21	5.79	18.49	65.77	686.93
	2011–2040	0.21	6.77	22.25	54.11	796.59
	2041–2070	0.19	7.42	25.09	64.39	879.51
	2071–2100	0.20	8.86	28.51	102.48	1024.03
Juneau	1981–2010	1.37	14.18	32.88	92.07	1747.05
	2011–2040	1.25	15.16	35.72	144.02	1816.60
	2041–2070	0.86	16.77	41.80	137.88	1963.05
	2071–2100	1.16	20.54	47.72	163.74	2353.02

amounts/percentages of precipitation extremes show a noticeable gradient from low latitude to the north polar Ocean (or coast) in Fig. 2.10c, d, for instance, along Urals (the longitude 60° E). Since these spatial patterns in daily maximum precipitation are mainly influenced by rainfall regimes and snowfall distributions, they are slightly different from general precipitation maps for the northern latitudes (Legates 1995; Adam and Lettenmaier 2003; Fekete et al. 2004).

Apart from the impact of regional climate patterns, the underestimation of gauge-measured daily maximum precipitation is also influenced by gauge catch efficiency. For instance, the catch efficiency of the Canadian Nipher snow gauge is much higher than the US NWS 8-inch standard gauge particularly for high wind speeds (Yang et al. 2005). Here we selected 480, 55, and 167 sites in Russia, the

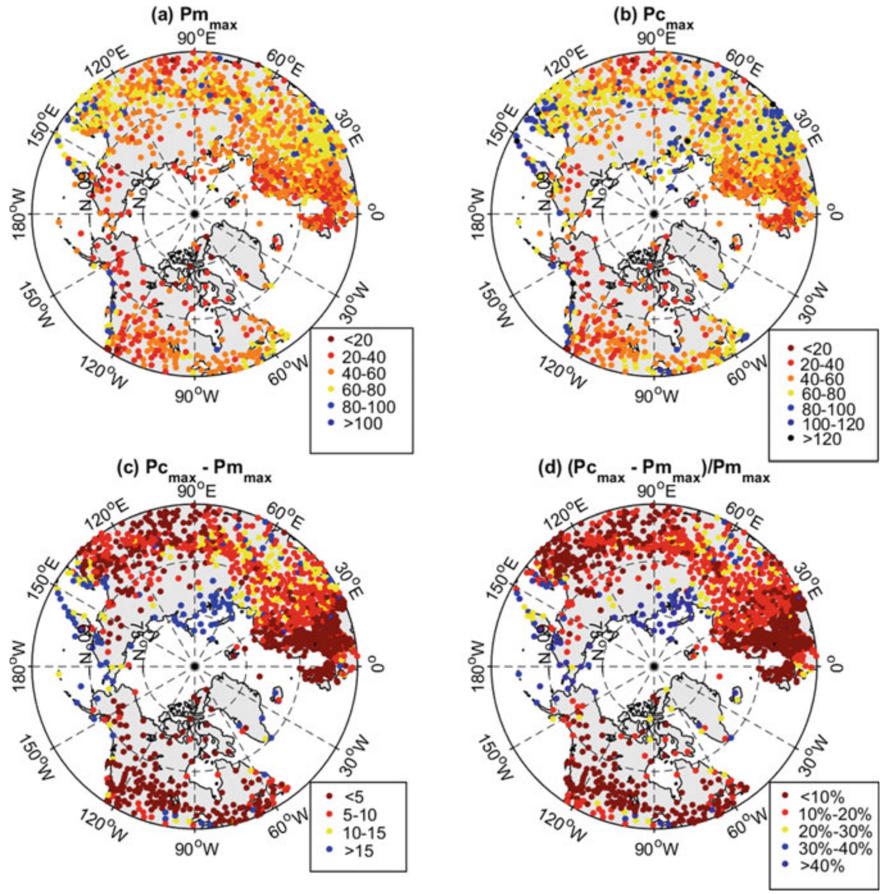

Fig. 2.10 Average of daily maximum precipitation for measured (**a**) and bias-corrected (**b**) data, respectively; average bias corrections of daily maximum precipitation (**c**); mean relative correction (**d**)

United States, and Canada, respectively, and impacts of gauge catch efficiency are shown by comparing minimum, maximum, and mean values of measured and corrected daily maximum precipitation at the sites in Fig. 2.11. Generally, the median values of minimum Pm_{max} and Pc_{max} are all no more than 20 mm in the three countries, while the median values of maximum Pm_{max} and Pc_{max} in Russia are much higher than the other two. This is mainly attributed to the regional climate difference. In addition, the United States and Canada are in the same region with comparable maximum and mean Pc_{max}, although maximum and mean Pm_{max} are all smaller in the United States. This indicates the correction factors play a significant role due to difference gauge catch efficiencies.

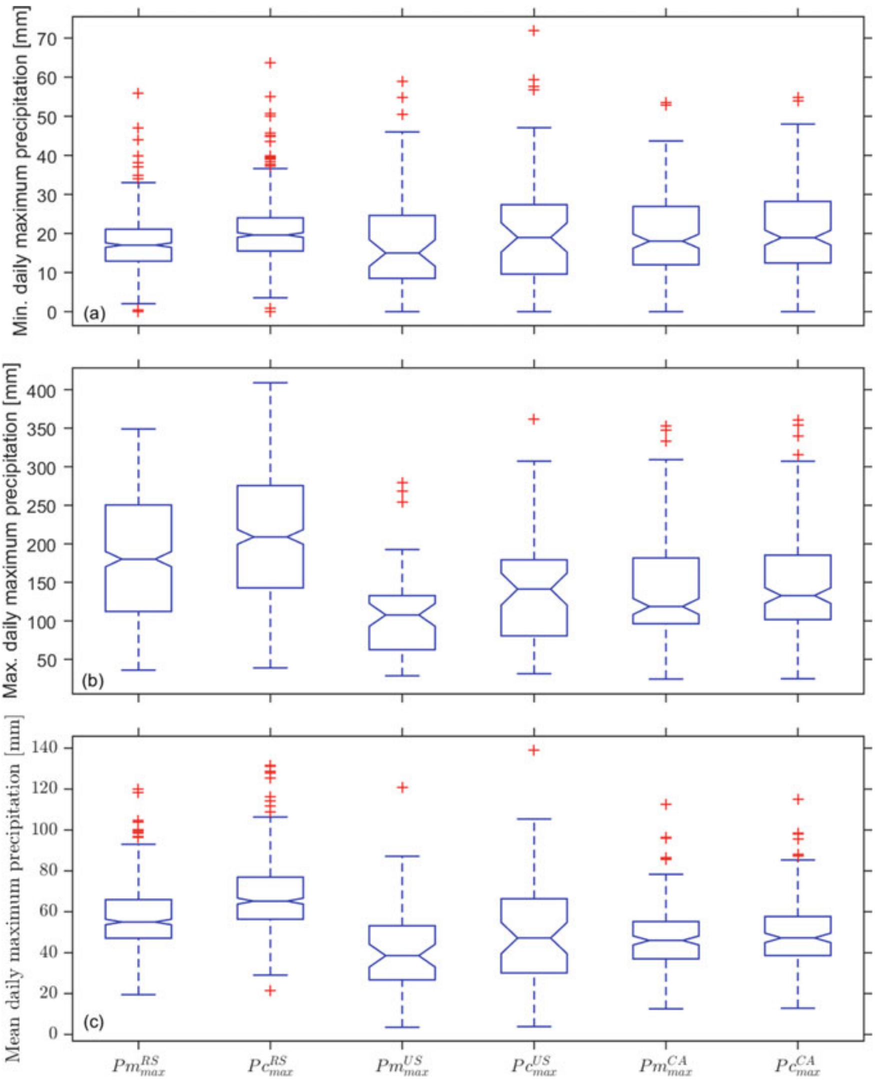

Fig. 2.11 Statistics of minimum (**a**), maximum (**b**), and mean (**c**) values of measured and corrected daily maximum precipitation at the sites in Russia, the United States, and Canada using different types of gauges. RS: Russia; US: United States; CA: Canada

2.5 Future Projection by Climate Models

Using state-of-the-art GCMs within the framework of CMIP5 to systematically quantify projected Arctic precipitation trends, Bintanja and Selten (2014) showed that the projected increases in Arctic precipitation over the twenty-first century, which peak in late autumn and winter, are due mainly to strongly intensified local surface evaporation, and only to a lesser degree to enhanced moisture inflow from lower latitudes. They also demonstrated that Arctic precipitation will continue to increase and possibly even accelerate in the twenty-first century with Arctic mean precipitation sensitivity of 4.5% increase per degree of temperature warming which is much larger than the global value (of 1–3%). Using a subset of the IPCC AR4 GCMs, Kattsov et al. (2007) have also showed that precipitation over the Arctic Ocean and its terrestrial watersheds, including the Ob, the Yenisey, the Lena, and the Mackenzie will increase through the twenty-first century, showing much faster percentage increases than global mean precipitation. The precipitation changes over the Arctic Ocean have also exhibited pronounced seasonality, with the strongest relative increase in winter and fall, and the weakest in summer (Kattsov et al. 2007). These are in general consistent with results for historical data records.

Based on the nine GCMs examined in the CMIP3, Rawlins et al (2010) calculated precipitation trends over the terrestrial Arctic basins during the 1950–2049 period ranging from 0.24 to as much as 0.92 mm/year, with the multi-model mean trend at 0.65 mm/year. Modeled results have also showed overall increases in snowfall and SWE associated with a projected increase in cold season precipitation in northeastern Eurasia and northern Canada, while they show decreases in more southerly locations where warming effects dominated, with the −10 and −20 °C late twentieth-century winter air temperature isotherm lines representing the transition boundaries for snowfall (Krasting et al. 2013; Deser et al. 2010) and SWE (Raisanen 2008) respectively.

Based on an ensemble-mean scenario, Barrow et al. (2014) have reported that the largest end-of-century increases in precipitation of 20–25% wetter are projected to occur in northern and eastern areas of Canada, while in more southerly regions precipitation increases are likely to be between 0 and 10% above 1961–1990 baseline conditions. They also observed large seasonal and spatial differences with projected increases in summer precipitation and decreases in winter precipitation in northern Canada while the reverse is true for the southern prairie provinces and British Columbia.

Summarizing various studies on projected changes in Canadian precipitation, Bush et al. (2016) concluded that, while projections of precipitation change are generally less robust and exhibit greater variability among models than those for temperature, increases in precipitation are projected for the majority of the country and for all seasons, the exception being parts of southern Canada where a decline in precipitation in summer and fall is projected.

After assessing projected changes to 1-, 2-, 3-, 5-, 7-, and 10-day annual maximum precipitation amounts over Canada, Mladjic et al. (2011) presented evidence that, while the Canadian Regional Climate Model (CRCM) underestimates precipitation extremes over most of Canada, when evaluated against observed changes, the northern Canadian climatic regions generally exhibit the highest percentage change in 20-, 50-, and 100-year return levels of precipitation extremes. Moreover, statistical frequency analysis of projected precipitation over the different regions of Canada by Mailhot et al (2010) suggests that daily and multi-day extreme precipitation events will be more intense and frequent in a future climate for all regions except the prairie provinces. In some regions (e.g., west coast of British Columbia), the return period associated with a given precipitation intensity in historical climate will decrease by a factor of five over the 2080–2100 period.

2.6 Concluding Remarks and Future Research

While precipitation represents one of the largest water fluxes in Arctic terrestrial hydrology, it is one of the most challenging variables to quantify at watershed scale due to the cold snow-dominated environment, limited in situ data, and heterogeneity of the landscape (e.g., Rawlins, et al. 2007). Similarly, Arctic terrestrial precipitation trends are inherently difficult to detect given snowfall measurement challenges resulting from gauge undercatch of solid precipitation, sparsely distributed observations, low precipitation amounts, and the scarcity of long-term records (Serreze and Hurst 2000; Adam and Lettenmaier 2003; Yang et al. 2005). The compounding effects of elevation on precipitation in topographically complex regions of the Arctic, where the distribution of observing stations is biased toward low elevations and coastal regions is also a factor.

Surface precipitation observation technologies are moving away from manual observations to automated stations. Joining manual and auto gauge observations are essential for the creation of longer time series. In order to avoid artificial discontinuity affecting the trend, proper transfer functions, adjustment using overlapping periods, and/or homogeneity testing should be applied. Further research is required for precipitation type and snowfall amount observations from in situ operational automatic stations.

Over the last four decades the emergence of remotely sensed data has enabled advances in retrieving precipitation rate, frequency, and spatial distribution over both land and ocean. The more recent instruments such as CloudSat, GPM core observatory, and GRACE together with advances in retrieval methods have provided added information that can further refine or constrain precipitation estimates in cold regions including high latitudes in the northern hemisphere. Other experiments such as the World Meteorological Organization (WMO) Solid Precipitation Intercomparison Experiment (SPICE) project (2013–2016) (Rasmussen et al. 2012; Kochendorfer et al. 2017) have also enhanced bias correction of in situ data in various climate regimes. These recent datasets collectively provide an unprecedented opportunity to advance estimation of precipitation amount, distribution, and changes in high latitudes, especially in the northern hemisphere where signals of change are robust. Therefore, more research in exploiting remote sensing techniques for measuring high-latitude precipitation and evapotranspiration should be pursued.

There are still systematic differences between precipitation in climate model simulations for the historical periods and considerable across-model scatter for future scenarios. While the range between individual model simulations is substantial, it is noteworthy that a comparable scatter exists even among different observational data (ACIA 2005). Research on examining climate model CMIP5' simulation on different types of precipitation show models overestimate non-convective precipitation and underestimate convective precipitation (Kusunoki and Arakawa 2015). One way to address these shortcomings is through the use of an Arctic regional climate system model that allows increased horizontal and vertical resolution and improved model physics that are optimized for polar regions (Maslowski et al. 2011).

Related to extreme short-duration rainfall projections, Zhang et al. (2017) state that it is challenging because of our poor understanding of its past and future behavior. The characterization of past changes is severely limited by the availability of observational data. Climate models, including typical regional climate models, do not directly simulate all extreme rainfall producing processes, such as convection. Recently developed convection-permitting models are better at simulating extreme precipitation, but this type of simulation is not yet widely available due to computational cost and possible uncertainties. Until better methods are available, the evidence observed from historical records and the relationship of the atmosphere's water-holding capacity with temperature still provide guidance for planners in extratropical regions, albeit with large uncertainties.

References

Adam JC, Lettenmaier DP (2003) Adjustment of global gridded precipitation for systematic bias. J Geophys Res 108(D9): 4257. https://doi.org/10.1029/2002JD002499

Adler RF et al (2003) The version-2 global precipitation climatology project (GPCP) monthly precipitation analysis (1979-present). J Hydrometeorology 4:1147–1167

Adler RF, Gu G, Huffman GJ (2012) Estimating climatological bias errors for the global precipitation climatology project (GPCP). J Appl Meteorol Climatol 51:84–99

Adler RF, Gu G, Sapiano M, Wang J-J, Huffman GJ (2017) Global precipitation: means, variations and trends during the satellite era (1979–2014). Surv Geophys 38:679–699

Alexander LV, et al. (2006) Global observed changes in daily climate extremes of temperature and precipitation. J Geophys Res 111:D05109. https://doi.org/10.1029/2005JD006290

Arctic Climate Impact Assessment (ACIA) (2005) Arctic climate impact assessment. Cambridge Univ. Press, New York, 1042 pp

Barrow E, Maxwell B, Gachon P (2004) Climate variability and change in Canada; past, present and future. Meteorological Service of Canada Environment Canada, Toronto

Behrangi A, Gardner A, Reager JT, Fisher JB, Yang D, Huffman GJ, Adler RF (2018) Using GRACE to estimate snowfall accumulation and assess gauge undercatch corrections in high latitudes. J Clim 31:8689–8704

Behrangi A, Gardner AS, Reager JT, Fisher JB (2017) Using GRACE to constrain precipitation amount over cold mountainous basins. Geophys Res Lett 44:219–227

Behrangi A et al (2016) Status of high-latitude precipitation estimates from observations and reanalyses. J Geophys Res: Atmos 121:4468–4486

Behrangi A, Imam B, Hsu KL, Sorooshian S, Bellerby TJ, Huffman GJ (2010) REFAME: rain estimation using forward-adjusted advection of microwave estimates. J Hydrometeorology 11:1305–1321

Behrangi A, Hsu K-I, Imam B, Sorooshian S, Huffman GJ, Kuligowski RJ (2009) PERSIANN-MSA: a precipitation estimation method from satellite-based multispectral analysis. J Hydrometeorology 10:1414–1429
Behrangi A, Lebsock M, Wong S, Lambrigtsen BH (2012) On the quantification of oceanic rainfall using spaceborne sensors. J Geophys Res 117:D20105
Behrangi A, Tian Y, Lambrigtsen BH, Stephens GL (2014a) What does CloudSat reveal about global land precipitation detection by other spaceborne sensors? Water Resour Res 50:4893–4905
Behrangi A, Wong S, Mallick K, Fisher JB (2014b) On the net surface water exchange rate estimated from remote-sensing observation and reanalysis. Int J Remote Sens 2170–2185
Berg W, L'Ecuyer T, Kummerow C (2006) Rainfall climate regimes: the relationship of regional TRMM rainfall biases to the environment. J Appl Meteorol Climatol 45:434–454
Bieniek PA, Walsh JE, Thoman RL, Bhatt US (2014) Using climate divisions to analyze variations and trends in Alaska temperature and precipitation. J Clim 27(8):2800–2818. https://doi.org/10.1175/JCLI-D-13-00342.1
Bieniek PA, Walsh JE (2017) Atmospheric circulation patterns associated with monthly and daily temperature and precipitation extremes in Alaska. Int J Climatol 37:208–217
Bintanja R, Selten FM (2014) Future increases in Arctic precipitation linked to local evaporation and sea-ice retreat. Nature 509:479–482. https://doi.org/10.1038/nature13259
Boening C, Lebsock M, Landerer F, Stephens GL (2012) Snowfall-driven mass change on the East Antarctic ice sheet. Geophys Res Lett 39:L21501
Bosilovich MG, Robertson FR, Chen J (2011) Global energy and water budgets in MERRA. J Clim 24:5721–5739
Brettschneider B, Trypaluk C (2014) Reexamination of the Alaska 1-Day record rainfall. Bull Am Meteor Soc 95(8):1249–1256. https://doi.org/10.1175/BAMS-D-13-00027.1
Brown RD, Braaten RO (1998) Spatial and temporal variability of Canadian monthly snow depths, 1946–1995. Atmos Ocean 36(1):37–54. https://doi.org/10.1080/07055900.1998.9649605
Bulygina ON, Razuvaev VN (2012) Daily temperature and precipitation data for 518 Russian meteorological stations. Carbon Dioxide Information Analysis Center, Oak Ridge National Laboratory, U.S. Department of Energy, Oak Ridge, Tennessee
Bush EJ, Loder JW, James TS, Mortsch LD, Cohen SJ (2014) An overview of Canada's changing climate. In: Lemmen DS (ed) Warren FJ. Canada in a changing climate, Sector Perspectives on Impacts and Adaptation, pp 23–64
Chamnansiri N (2016) Changes in precipitation characteristics associated with air temperature, dew point temperature and relative humidity over southeastern Canada during 1977–2015. MA thesis, California State University, Los Angeles. http://hdl.handle.net/10211.3/173880
Collins M et al (2013) Long-term climate change: projections, commitments and irreversibility. In Stocker TF et al (eds) Climate change 2013: the physical science basis. Cambridge University Press, 1029–1136
Colony R, Randinov V, Tanis FR (1998) Measurements of precipitation and snow pack at Russian north pole drifting stations. Polar Record 34(188):3–14
Dee DP et al (2011) The ERA-interim reanalysis: configuration and performance of the data assimilation system. Q J R Meteorol Soc 137:553–597
Deser C, Tomas R, Alexander M, Lawrence D (2010) The seasonal atmospheric response to projected Arctic sea ice loss in the late 21st century. J Clim 23:333–351. https://doi.org/10.1175/2009JCLI3053.1
Dingman SL (2008) Physical hydrology, 2nd edn. Waveland Press, Long Grove, IL, p 646
Dirmeyer PA, Jin Y, Singh B, Yan X (2013) Trends in land–atmosphere interactions from CMIP5 simulations. J Hydrometeorology 14(3):829–849
Donat MG, Lowry AL, Alexander LV, O'Gorman PA, Maher N (2017) Addendum: More extreme precipitation in the world's dry and wet regions. Nat Clim Change 7(2):154–158

Draper DW, Newell DA, Wentz FJ, Krimchansky S, Skofronick-Jackson GM (2015) The Global Precipitation Measurement (GPM) Microwave Imager (GMI): Instrument Overview and Early On-Orbit Performance. IEEE J Sel Top Appl Earth Obse Remote Sens 8(7):3452–3462

Fekete BM, Vörösmarty CJ, Roads JO, Willmott CJ (2004) Uncertainties in precipitation and their impacts on runoff estimates. J Clim 17:294–304

Ferraro RR et al (2013) An Evaluation of Microwave Land Surface Emissivities Over the Continental United States to Benefit GPM-Era Precipitation Algorithms. IEEE Trans Geosci Remote Sens 51:378–398

Førland EJ, Hanssen-Bauer I (2003) Past and future climate variations in the Norwegian Arctic: overview and novel analysis. Polar Res 22(2):113–124. https://doi.org/10.1111/j.1751-8369.2003.tb00102.x

Fuchs T, Rapp J, Rubel F, Rudolf B (2001) Correction of synoptic precipitation observations due to systematic measuring errors with special regard to precipitation phases. Phys Chem Earth Part B 26:689–693

Goodison BE, Louie PYT, Yang D (1998) WMO solid precipitation measurement intercomparison. Rept 67:212 pp. World Meteorological Organization, Geneva

Goodison BE, Louie PYT, Yang D (1988) WMO solid precipitation measurement intercomparison, final report, WMO/TD-No. 872, WMO, Geneva, 212 pp

Groisman PY, Rankova EY (2001) Precipitation trends over the Russian permafrost-free zone: removing the artfacts of pre-professing. Inter J Climatol 21:657–678

Groisman PY, Knight RW, Easterling DR, Karl TR (2005) Trends in intense precipitation in climate record. J Climate 18:1326–1350

Groisman PYa, Koknaeva VV, Belokrylova TA, Karl TR (1991) Overcoming biases of precipitation measurement: a history of the USSR experience. Bull Amer Meteor Soc 72:1725–1733. https://doi.org/10.1175/1520-0477(1991)072%3c1725:OBOPMA%3e2.0CO;2

Groisman PYa, Sun B, Vose RS, Lawrimore JH, Whitfield PH, Serreze MC, Razuvaev V, Alekseev G (2003) Contemporary Climate Changes in High Latitudes of the Northern Hemisphere: Daily Time Resolution. In Proceedings of the 14th symposium on global change and climate variations, 1–10. Long Beach, CA: American Meteorological Society

Hsu KL, Gao XG, Sorooshian S, Gupta HV (1997) Precipitation estimation from remotely sensed information using artificial neural networks. J Appl Meteorol 36:1176–1190

Huffman GJ et al (2001) Global precipitation at one-degree daily resolution from multisatellite observations. J Hydrometeorology 2:36–50

IPCC (2013) Climate Change 2013: The Physical Science Basis. Report of Working Group I of the Intergovernmental Panel on Climate Change. Cambridge University Press, Cambridge, U.K

Jarujareet P (2016) Precipitation trends under a warming climate in British Columbia, Canada, from 1950–2010. MA Thesis, California State University, Los Angeles. http://hdl.handle.net/10211.3/173903

Kane DL, Stuefer SL (2013) Challenges of Precipitation Data Collection in Alaska. 19th International Northern Research Basins Symposium and Workshop Southcentral Alaska, USA —August 11–17, 2013

Kattsov VM et al (2007) Simulation and Projection of Arctic Freshwater Budget Components by the IPCC AR4 Global Climate Models. J of Hydrometeorology 8(3):571–589

Kochendorfer J, Nitu R, Wolff M, Mekis E, et al. (2017) Errors and adjustments for single-Alter shielded and unshielded weighing gauge precipitation measurements from WMO-SPICE. Hydrol Earth Syst Sci Discuss. https://doi.org/10.5194/hess-2016-684, in review

Kopec BG, eng X, Michel FA, Posmentier ES (2015) Influence of sea ice on Arctic precipitation. Proc Natl Acad Sci 113(1):46–51. https://doi.org/10.1073/pnas.150463133

Korzun VI (Editor-in-Chief) (1978) World water balance and water resources of the earth. Unesco Press, Paris, pp 663

Krasting JP, Broccoli AJ, Dixon KW, Lanzante JR (2013) Future changes in northern hemisphere snowfall. J Clim 26(20):7813–7828

Kuligowski RJ (2002) A self-calibrating real-time GOES rainfall algorithm for short-term rainfall estimates. J Hydrometeorology 3:112–130

Kummerow C, Barnes W, Kozu T, Shiue J, Simpson J (1998) The Tropical Rainfall Measuring Mission (TRMM) sensor package. J Atmo Oceanic Technol 15:809–817

Kummerow CD, Randel D, Petkovic V (2016) Results from GPM GPROF V4 and improvements planned for V5, 8th IPWG and 5th IWSSM joint workshop bologna, 3–7 October, 2016. http://www.isac.cnr.it/~ipwg/meetings/bologna-2016/Bologna2016_Posters/P1-20_Kummerow.pdf

Kummerow CD, Randel DL, Kulie M, Wang N, Ferraro R, Munchak SJ, Petkovic V (2015) The evolution of the Goddard profiling algorithm to a fully parametric scheme. J Atmos Oceanic Technol 32:2265–2280

Kusunoki S, Arakawa O (2015) Are CMIP5 models better than CMIP3 models in simulating precipitation over East Asia? J Clim 28:5601–5621

Lader R, Walsh JE, Bhatt US, Bieniek PA (2017) Projections of twenty-first-century climate extremes for Alaska via dynamical downscaling and quantile mapping. J Appl Meteor Climatol 56:2393–2409. https://doi.org/10.1175/JAMC-D-16-0415.1

Lau WK, Wu MHT, Kim KM (2013) A canonical response of precipitation characteristics to global warming from CMIP5 models. Geophys Res Lett 40:3163–3169

Lebsock MD, L'Ecuyer TS (2011) The retrieval of warm rain from CloudSat. J Geophys Res 116: D20209

Legates DR, Willmott CJ (1990) Mean seasonal and spatial variability in gauge-corrected, global precipitation. Internat J Climatol 10:111–127

Legates DR (1995) Global and terrestrial precipitation: a comparative assessment of existing climatologies. Int J Climatol 15:237–258

Liu G (2008) Deriving snow cloud characteristics from CloudSat observations. J Geophys Res 113:D00A09

Lydolph PE (1977) Climates of the Soviet Union. World survey of climatology volume 7, Elsevier Scientific Publishing Company, Amstrerdam-Oxford-New York

Mailhot A, Kingumbi A, Talbot G, Poulin A (2010) Future changes in intensity and seasonal pattern of occurrence of daily and multi-day annual maximum precipitation over Canada. J Hydrol 388(3):173–185

Maslowski W, Cassano J, Gutowski W, Lettenmaier D (2011) Regional arctic climate system model (RACM) - development and selected results, geophysical research abstracts, 13, EGU2011-9648, 2011, EGU General Assembly

Metcalfe JR, Routledge B, Devine K (1997) Rainfall measurement in Canada: changing observational methods and archive adjustment procedures. J. Clim 10:92–101

McAfee S, Guentchev G, Eischeid J (2013) Reconciling precipitation trends in Alaska: 1. Station-based analyses. J Geophys Rese 118:7523–7542. https://doi.org/10.1002/jgrd.50572

McAfee S, Guentchev G, Eischeid J (2014) Reconciling precipitation trends in Alaska: 2. Gridded data analyses. J Geophys Res. https://doi.org/10.1002/2014jd022461

Mekis É (2005) Adjustments for trace measurements in Canada. In 15th conference on applied climatology, Savannah, Georgia, USA, June, J3.7 (pp 20–24)

Mekis É, Vincent LA (2011) An overview of the second generation adjusted daily precipitation dataset for trend analysis in Canada. Atmos.–Ocean, 49, 163–177, https://doi.org/10.1080/07055900.2011.583910

Mekis É, Brown R (2010) Derivation of an adjustment factor map for the estimation of the water equivalent of snowfall from ruler measurements in Canada. Atmos Ocean 48(4):284–293

Mekis E, Vincent LA (2011b) An overview of the second generation adjusted daily precipitation dataset for trend analysis in Canada. Atmos Ocean 49:163–177

Mladjic B, Sushama L, Khaliq MN, Laprise R, Caya D, Roy R (2011) Canadian RCM projected changes to extreme precipitation characteristics over Canada. J Clim 24(10):2565–2584

Montenegro F (2015) A look into changes in precipitation types linked with surface air temperature over British Columbia, Canada 1953–2005. MA thesis, California State University, Los Angeles. http://hdl.handle.net/10211.3/133589

Pendergrass AG, Lehner F, Sanderson BM, Xu Y (2015) Does extreme precipitation intensity depend on the emissions scenario? Geophys Res Lett 42:8767–8774

Peel MC, Finlayson BL, McMahon TA (2007) Updated world map of the Köppen –Geiger climate classification. Hydrol Earth Syst Sci 11:1633–1644

Perica S, Kane D, Dietz S, Maitaria K, Martin D, Pavlovic S, Roy I (2012) NOAA Atlas 14: Precipitation- frequency atlas of the United States, Alaska. www.nws.noaa.gov/oh/hdsc/PF_documents/Atlas14_Volume7.pdf

Ponce M (2017) Detecting climate change over Canadian prairies. MA thesis at California State University, Los Angeles http://hdl.handle.net/10211.3/192086

Räisänen J (2008) Warmer climate: less or more snow? Clim Dyn 30:307–319. https://doi.org/10.1007/s00382-007-0289-y

Rapaić M, Brown R, Markovic M, Chaumont D (2015) An evaluation of temperature and precipitation surface-based and reanalysis datasets for the Canadian Arctic, 1950–2010. Atmos Ocean 53(3):283–303

Rasmussen R, Baker B, Kochendorfer J (2012) How well are we measuring snow: The NOAA/FAA/NCAR winter precipitation test bed. Bull Amer Mete Soc 93:811–829

Rawlins MA, Fahnestock M, Frolking S, Vörösmarty CJ (2007) On the evaluation of snow water equivalent estimates over the terrestrial Arctic drainage basin. Hydrol Process 21:1616–1623

Rawlins MA et al (2010) Analysis of the arctic system for freshwater cycle intensification: Observations and expectations. J Clim 23:5715–5737

Scaff L, Yang D, Li Y, Mekis E (2015) Inconsistency in precipitation measurements across the Alaska-Yukon border. The Cryosphere 9:2417–2428

Schneider U, Finger P, Meyer-Christoffer A, Rustemeier E, Ziese M, Becker A (2017) Evaluating the hydrological cycle over land using the newly-corrected precipitation climatology from the global precipitation climatology centre (GPCC). Atmosphere 8:52

Serreze MC, Etringer AJ (2003) Precipitation charactersitics of the Eurasian Arctic Drainage system. Inter J Climatol 23:1267–1291

Serreze MC, Hurst CM (2000) Representation of mean Arctic precipitation from NCEP-NCAR and ERA reanalyses. J Clim 13:182–201

Shephard MW, Mekis E, Morris RJ, Feng Y, Zhang X, Kilcup K, Fleetwood R (2014) Trends in canadian short-duration extreme rainfall: including an intensity–duration–frequency perspective. Atmos Ocean 52(5):398–417

Short DA, Nakamura K (2000) TRMM radar observations of shallow precipitation over the tropical oceans. J Clim 13:4107–4124

Shulski M, Wendler G2 (2007) Climate of Alaska. University of Alaska Press

Skofronick-Jackson G et al (2017) The global precipitation measurement (GPM) mission for science and society. Bull Am Meteor Soc 98:1679–1695

Smith LC, Sheng Y, MacDonald GM, Hinzman LD (2005) Disappearing arctic lakes. Science 308:1429

Solomon S et al (2007) Technical summary, in climate change 2007: the physical science basis. In: S. Solomon et al (ed) Contribution of working group I to the fourth assessment report of the intergovernmental panel on climate change. Cambridge Univ. Press, Cambridge, UK, pp 20–91

Sorooshian S, Hsu KL, Gao X, Gupta HV, Imam B, Braithwaite D (2000) Evaluation of PERSIANN system satellite-based estimates of tropical rainfall. Bull Am Meteor Soc 81:2035–2046

Stephens GL et al (2008) CloudSat mission: performance and early science after the first year of operation. J Geophys Res: Atmos 113:D00A18

Stuefer SL, Kane DL (2016) Snow retention for increased water supply of shallow arctic lakes. Cold Reg Sci Technol 123(March):32–43. https://doi.org/10.1016/j.coldregions.2015.11.011

Stuefer SL, Kane DL, Liston GE (2013) In situ snow water equivalent observations in the US arctic. Hydrol Res 44(1):21. https://doi.org/10.2166/nh.2012.177

Stuefer SL, Arp C, Kane DL, Liljedahl A (2017) Recent extreme runoff observations from coastal Arctic watersheds in Alaska. Water Resour Res 53(11):9145–9163

Sturm M, Stuefer SL (2013) Wind-blown flux rates derived from drifts at arctic snow fences. J Glaciol 213(59):21–34. https://doi.org/10.3189/2013JoG12J110

Swenson S (2010) Assessing high-latitude winter precipitation from global precipitation analyses using GRACE. J Hydrometeorology 11:405–420

Tapley BD, Bettadpur S, Ries JC, Thompson PF, Watkins MM (2004) GRACE measurements of mass variability in the earth system. Science 305:503–505

Tebaldi C, Arblaster JM, Hayhoe K, Meehl GA (2006) Going to the extremes: an intercomparison of model-simulated historical and future changes in extreme events. Clim Change 79:185–211. https://doi.org/10.1007/s10584-006-9051-4

USGCRP (2014) US national climate assessment, 2014: global climate change impacts in the United States. US.Global Change Research Program, Washington, DC. http://nca2014.globalchange.gov/downloads

Vincent LA, Mekis E (2009) Discontinuities due to joining precipitation station observations in Canada. J Appl Meteorol Climatol 48(1):156–166

Vincent LA, Zhang X, Brown RD, Feng Y, Mekis E, Milewska EJ, Wan H, Wang XL (2015) Observed trends in Canada's climate and influence of low-frequency variability modes. J Clim 28(11):4545–4560

Vincent LA, Mekis E (2006) Changes in daily and extreme temperature and precipitation indices for Canada over the twentieth century. Atmos Ocean 44(2):177–193

Vincent LA, Wang XL, Milewska EJ, Wan H,Yang F, Swail V (2012) A second generation of homogenized Canadian monthly surface air temperature for climate trend analysis. J Geophys Res: Atmos 117(D18). https://doi.org/10.1029/2012jd017859

Walsh JE, Kattsov V, Portis D, Meleshko V (1988) Arctic precipitation and evaporation: model results and observational estimates. J. Clim 11(1):72–87

Walsh JE, Kattsov V, Portis D, Meleshko V (1998) Arctic precipitation and evaporation: model results and observational estimates. J Clim 11:72–87

Watkins MM, Wiese DN, Yuan D-N, Boening C, Landerer FWCJB (2015) Improved methods for observing Earth's time variable mass distribution with GRACE using spherical cap mascons. J Geophys Res: Solid Earth 120:2648–2671

Wilheit TT (1986) Some comments on passive microwave measurement of rain. Bull Am Meteor Soc 67:1226–1232

Xie P, Arkin PA (1997) Global precipitation: A 17-Year monthly analysis based on gauge observations, satellite estimates, and numerical model outputs. Bull Am Meteor Soc 78:2539–2558

Yang D et al (2001) Compatibility evaluation of national precipitation gage measurements. J Geophys Res: Atmos 106:1481–1491

Yang D, Goodison BE, Metcalfe JR, Golubev VS, Elomaa E, Gunther TH, Bates R, Pangburn TC, Hanson L, Emerson D, Copaciu V, Milkovic J (1995) Accuracy of Tretyakov precipitation gauge: results of WMO Intercomparison. Hydrol Process 9(8):877–895

Yang D (1999) An improved precipitation climatology for the arctic ocean. Geophys Res Lett 26 (11):1625–1628

Yang D, Kane D, Zhang Z (2005) Bias corrections of long-term (1973–2004) daily precipitation data over the northern regions. Geophys Res Lett 32:L19501. https://doi.org/10.1029/2005GL024057

Yang D, Goodison BE, Metcalfe JR, Golubev VS, Bates R, Pangburn T, Hanson CL (1998) Accuracy of NWS 8″ standard nonrecording precipitation gauge: results and application of WMO intercomparison. J Atmos Oceanic Technol 15(1):54–68

Ye H, Cohen J (2013) Shortening snowfall season associated with increasing air temperature over northern Eurasia. Environ ResLett 8(2013)014052. http://stacks.iop.org/1748-9326/8/014052

Ye H (2001) Characteristics of winter precipitation variation over Northern Central Eurasia and their connections to sea surface temperatures over the Atlantic and Pacific oceans. J Clim 14:3140–3155

Ye H (2008) Changes in frequency of precipitation types associated with surface air temperature over Northern Eurasia during 1936-90. J Clim 21:5807–5819. https://doi.org/10.1002/joc.1741
Ye H, Fetzer EJ (2010) Atmospheric moisture content associated with surface air temperatures during northern Eurasian summer. Int J Climatol 30(10):1463–1471. https://doi.org/10.1002/joc.1991
Ye H, Fetzer EJ, Wong S, Behrangi A, Olsen ET, Cohen J, Lambrigtsen BH, Chen L (2014) Impact of increased water vapor on precipitation efficiency over northern Eurasia. Geophys Res Lett 41:2941–2947. https://doi.org/10.1002/2014GL,059830
Ye H, Fetzer EJ, Wong S, Yang D, Lambrigtsen BH (2015) Increasing atmospheric water vapor and higher daily precipitation intensity over Northern Eurasia. Geophys Res Lett 42 https://doi.org/10.1002/2015GL066104
Ye H, Fetzer EJ, Behrangi A, Wong S, Lambrigtsen BH, Wang CY, Cohen J, Gamelin BL (2016a) Increasing daily precipitation intensity associated with warmer air temperatures over Northern Eurasia. J Clim 29:623–636
Ye H, Fetzer EJ, Wong S, Lambrigtsen BH, Wong T, Chen L, Dang V (2016b) More frequent showers and thunderstorm events under a warming climate: evidence observed over Northern Eurasia from 1966–2000. Clim Dyn, 13 pp. https://doi.org/10.1007/s00382-016-3412-0
Ye H, Fetzer EJ, Wong S, Lambrigtsen BH (2017) Rapid decadal convective precipitation increase during the last three decades of the 20th century. Sci Adv 3:1600944
Zhang X, Harvey KD, Hogg WD, Yuzyk TR (2001) Trends in Canadian streamflow. Water Resour Res 37:987–998 https://doi.org/10.1029/2000WR900357
Zhang X, Zwiers FW, Li G, Wan H, Cannon AJ (2017). Complexity in estimating past and future extreme short-duration rainfall. Nat Geosci 10(4):255–259
Zolina, O, Simmer C, Gulev SK, Kollet S (2010) Changing structure of European precipitation: longer wet periods leading to more abundant rainfalls. Geophys Res Letts 37:L06704. https://doi.org/10.1029/2010GL042468

Dr. Hengchun Ye is the Associate Dean of Natural and Social Sciences at California State University, Los Angeles, USA. She was a Professor and Department Chair in the Department of Geosciences and Environment and the PI for NASA DIRECT-STEM at the Cal State LA. Her research focuses on hydroclimatology and climate change. Her research expertise is in changing precipitation characteristics (intensity, frequency, and type), durations of wet and dry days, and snow (snowfall season length and accumulation) and its connections to atmospheric water vapor, atmospheric circulation patterns, and sea surface temperatures. She received her Ph.D. in Climatology at the University of Delaware and held tenure-track positions at the University of Idaho and Emporia State University before she took an associate professor position at Cal State LA.

Dr. Daqing Yang is a Research Scientist at the Watershed Hydrology and Ecology Research Division, Environment and Climate Change Canada. He is also Affiliate Research Professor at the International Arctic Research Center, Univ. of Alaska Fairbanks. Over the past 25 years, he has conducted cryosphere system research in China, Canada, Japan, USA, and Norway. His primary research activities/interests include cold region hydrology and climate, particularly Arctic large river streamflow regime and change, snow cover and snowfall measurements, climate change and human impact to regional hydrology, and applications of remote sensing in cold regions. He has served as journal editor and subject editor for IAHS publications (cold region hydrology, northern research basin water balance, and cold/mountain region hydrological systems under climate change), and WMO technical reports (solid precipitation measurement intercomparison and integrated global observing strategy cryosphere theme). He also contributed as review and/or author to the IPCC Reports, and the Arctic Council's Snow, Water, Ice and Permafrost in the Arctic (SWIPA 2017 and follow up) assessment. His current research focuses on investigating the impacts of climate variability/change and human activities on hydrologic system across the broader northern regions.

Dr. Ali Behrangi is an Associate Professor in the Department of Hydrology and Atmospheric Sciences and also Department of Geosciences, University of Arizona, USA. His research interest and activities are in various aspects of cloud-precipitation and hydrologic studies: Retrieval, diagnostic evaluation, and uncertainty analysis of precipitation products, extreme weather event analysis, and hydrologic simulations. In the last 7 years, he has had a greater focus on remote sensing of precipitation in cold regions, where he has also utilized CloudSat, GRACE, reanalyses, and other new observations. He currently leads a project to improve GPCP in high latitudes. He received his Doctoral degree in Civil Engineering at University of California, Irvine and was a postdoctoral scholar at California Institute of Technology (Caltech). He was with NASA JPL as Scientist for more than 5 years (2013–2018), before he joined the University of Arizona.

Dr. Svetlana L. Stuefer is an Associate Professor at the Department of Civil and Environmental Engineering and Water and Environmental Research Center at the University of Alaska Fairbanks, Alaska, USA. Her specialization is in the cold region's hydrology with an emphasis on the snow and ice-related processes. She received her Ph.D. from the Russian State Hydrometeorological University, St. Petersburg, Russia. She joined the Water and Environmental Research Center at the University of Alaska Fairbanks in 2003 as a Postdoctoral Fellow. Her research can be viewed at ORCID https://orcid.org/0000-0003-0740-8335.

Dr. Xicai Pan is a Professor in the State Key Laboratory of Soil and Sustainable Agriculture, Institute of Soil Science, Chinese Academy of Sciences, in Nanjing, China. He studies soil and terrestrial environmental physics and associated ecosystem services. His research includes investigations of key processes affecting cold region hydrology and the sustainability of agricultural ecosystems. He received his doctoral degree in Environmental Physics at the Heidelberg University in Germany, and was a Postdoctoral Fellow at the University of Saskatchewan in Canada.

Dr. Eva Mekis is a Physical Scientist in the Meteorological Research Division of Environment and Climate Change Canada in Toronto, Ontario, Canada. She graduated and received her Doctoral degree in Meteorology at the Eötvös Loránd University in Budapest (Hungary). Since arriving in Canada as an NSERC Postdoctoral fellow, she spent over 20 years dealing with precipitation-related issues. Her main research interest includes the development of precipitation data adjustment and homogenization procedures and the analysis of precipitation-related climate indices and trends. She developed and maintaining the first and second generation of the Adjusted Historical Canadian Climate Data (AHCCD) precipitation database used by thousands of applications and users. Recently, her focus shifted toward the automated precipitation observations including observation data flow, quality control, catch efficiency assessment, and transfer function development.

Dr. Yonas Dibike is a Research Scientist at Environment and Climate Change Canada, Watershed Hydrology and Ecology Research Division at the University of Victoria. His research interests include hydrological, hydrodynamic, and transport modeling as well as hydro-climate analysis and climate change impact studies in cold region watersheds. He also holds adjunct faculty appointment at McMaster University, and the University of Victoria in Canada. He is the author/co-author of numerous (70) scientific articles that have appeared in a variety of peer-reviewed journals and conference proceedings. He is actively involved in Departmental and University-based researches and has co-supervised several graduate students and post-doctoral fellows.

Dr. John E. Walsh is the Chief Scientist of the International Research Center and President's Professor of Global Change at the University of Alaska, Fairbanks, USA. He is also an emeritus faculty member of the University of Illinois. He has been involved in Arctic research and education for more than 40 years. His more recent research has addressed Arctic climate and weather variability, with an emphasis on the drivers of cryospheric variations over seasonal to multidecadal timescales. He has served as lead author for assessment reports of the Intergovernmental Panel on Climate Change, the Arctic Monitoring and Assessment Programme, and the U.S. National Climate Assessment. He has also co-authored a textbook, Severe and Hazardous Weather. He received a B.S. in Mathematics from Dartmouth College and a Ph.D. in Meteorology from the Massachusetts Institute of Technology.